NASA TECHNICAL NOTE

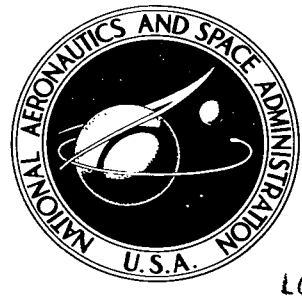

NASA TN D-3056

NASA TN D-3056

THRUST COEFFICIENTS OF LOW-THRUST NOZZLES

by Ernie W. Spisz, Paul F. Brinich, and John R. Jack

Lewis Research Center
Cleveland, Ohio

NATIONAL AERONAUTICS AND SPACE ADMINISTRATION • WASHINGTON, D. C. • OCTOBER 1965

THRUST COEFFICIENTS OF LOW-THRUST NOZZLES

By Ernie W. Spisz, Paul F. Brinich, and John R. Jack

Lewis Research Center
Cleveland, Ohio

NATIONAL AERONAUTICS AND SPACE ADMINISTRATION

For sale by the Clearinghouse for Federal Scientific and Technical Information
Springfield, Virginia 22151 – Price $2.00

THRUST COEFFICIENTS OF LOW-THRUST NOZZLES

by Ernie W. Spisz, Paul F. Brinich, and John R. Jack

Lewis Research Center

SUMMARY

The performance losses associated with small nozzles operating at low propellant flow rates were investigated experimentally with a resistance-heated hydrogen thrustor. Data were obtained for seven different nozzles covering the range of nozzle area ratio from 25 to 150, hydrogen propellant flow rates of 0.5×10^{-4}, 1.0×10^{-4}, and 2.5×10^{-4} pound per second, and propellant temperatures from 530° to 4000° R.

The nozzle losses, as determined by the difference between the one-dimensional isentropic thrust coefficient and the measured thrust coefficient, were correlated in terms of the throat Reynolds number and nozzle area ratio. At low throat Reynolds number, the nozzle losses were sufficiently large to result in measured thrust coefficients less than the values calculated for isentropic flow through a choked orifice. Results show that large area ratios are not required for achieving maximum thrust for nozzles with low throat Reynolds number (<10 000).

INTRODUCTION

It has been generally recognized (refs. 1 and 2) that viscous boundary-layer and heat-transfer effects on the divergent surfaces of supersonic nozzles can degrade the performance (thrust, specific impulse, and efficiency) of low-thrust thermal-propulsion devices. The performance losses associated with these nozzle-expansion effects have not been of immediate concern because they are negligible for the relatively high thrust levels (>500 millipounds) of thrustors that are being developed. The experimental performance values of these thrustors are generally within a few percent of the calculated values for a one-dimensional isentropic nozzle-expansion process. (Typical one-dimensional isentropic nozzle-expansion calculations for hydrogen are presented in refs. 3 and 4.) However, for lower thrust levels (<100 millipounds, which may be desirable for applications such as attitude control of space vehicles) the boundary-layer and

heat-transfer effects that occur in the divergent portion of the nozzle become more pronounced. For such small, low-thrust nozzles, the boundary layer can account for a substantial portion of the available nozzle flow area. The boundary layer introduces viscous losses and alters the free-stream conditions so that the conventional assumption of a one-dimensional isentropic expansion process becomes questionable. The nozzle flow is further modified as a result of the thermal boundary layer and the corresponding heat-transfer effects that are intimately coupled to both the free-stream and boundary-layer flows. For low propellant flow rates, heat-transfer losses to the nozzle walls can be a significant portion of the total thermal energy available for conversion to kinetic energy.

Little experimental data are available for estimating the boundary-layer and heat-transfer losses at low-thrust levels. Some overall performance data are presented in references 5 and 6, but these data primarily indicate only the performance losses that can occur at low-thrust levels. The program herein was undertaken to study further the nozzle losses from performance data obtained with the radiation-cooled resistojet of reference 7. Previous experience with this radiation-cooled resistojet at low-thrust levels had indicated that, as the propellant flow rate was decreased corresponding to a reduction in thrust level, the thrust coefficient also decreased. This decrease in thrust coefficient was interpreted in terms of a Reynolds number effect. This effect is investigated herein and covers nozzle throat Reynolds numbers ranging approximately from 500 to 18 000. This range was obtained by varying propellant flow rate, nozzle throat diameter, and viscosity (by propellant temperature changes). The effects of nozzle area ratio were studied for seven different nozzles with area ratios ranging from 25 to 150. All nozzle divergent sections were conical and had a divergence angle of 20°. Hydrogen was used exclusively as the propellant, and data were obtained for propellant temperatures ranging from 530° to 4000° R.

PERFORMANCE CONSIDERATIONS

For a conical nozzle such as that shown in figure 1, the thrust that would be developed in a vacuum environment is given by

$$F = \int_0^{r_e} \frac{2\pi\rho_e}{g}(u_e)_x^2 r\, dr + \int_0^{r_e} 2\pi p_e r\, dr \qquad (1)$$

(All symbols are defined in appendix A.)

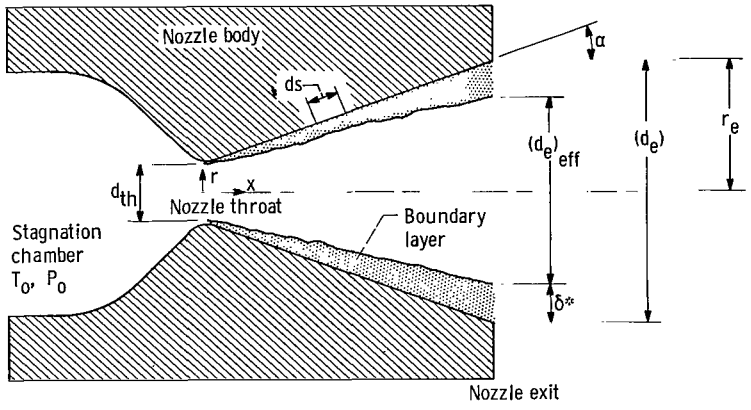

Figure 1. - Schematic drawing of nozzle.

For a one-dimensional isentropic expansion process, equation (1) can be integrated and the thrust given by (ref. 8)

$$F_i = \frac{\dot{w}}{g} u_e \lambda + p_e A_e \tag{2}$$

where λ is the nozzle angle divergence coefficient, $\lambda = \frac{1}{2}(1 + \cos \alpha)$.

If the thrust is nondimensionalized to obtain the thrust coefficient $C_F \equiv F/P_o A_{th}$, the following equation for the thrust coefficient, in terms of the nozzle area ratio, propellant specific heat ratio, and nozzle divergence angle, results:

$$C_{F_i} \equiv \frac{F_i}{P_o A_{th}} = \lambda\gamma \left\{ \left(\frac{2}{\gamma-1}\right)\left(\frac{2}{\gamma+1}\right)^{\frac{\gamma+1}{\gamma-1}} \left[1 - \left(\frac{p_e}{P_o}\right)^{\frac{\gamma-1}{\gamma}} \right] \right\}^{1/2} + \frac{p_e}{P_o} \frac{A_e}{A_{th}} \tag{3}$$

To calculate the thrust for a nonisentropic and non-one-dimensional nozzle-expansion process, equation (1) requires that the distribution of density, velocity, and pressure at the nozzle exit be known. If this information is unavailable, it is necessary to resort to approximate calculation techniques. A technique often used is to define the thrust as the difference between the calculated isentropic thrust and an estimated thrust-loss term:

$$F = F_i - F_\ell \tag{4}$$

For small nozzles, the thrust-loss term is composed primarily of viscous drag on the divergent surfaces of the nozzle and heat-transfer losses incurred during the expansion process:

$$F_\ell = F_v + F_{ht} \tag{5}$$

The thrust loss due to heat-transfer losses to the nozzle walls F_{ht} can be estimated for a specific nozzle geometry, cooling design, and operating condition. This loss, however, is minor for radiation-cooled thrustors except at very low propellant flow rates and therefore will not be evaluated here. The thrust loss due to viscous effects F_v is given by the integral of the local shear stress τ over the divergent surfaces of the nozzle:

$$F_v = \int_s 2\pi r \tau \cos \alpha \, ds \tag{6}$$

The magnitude of this loss can be estimated by assuming that the local shear stress is given by the skin friction relation for laminar flow over a flat plate (ref. 9). Although the laminar flat plate relation does not apply directly to axisymmetric nozzle flow with its inherent axial variations in the flow conditions and possible turbulence, the resulting estimates provide a simple first approximation for the comparison with experiment.

With this assumption, the loss in thrust coefficient due to viscous drag on the surface of a conical nozzle was derived in appendix B and is given by

$$C_{F_v} = \frac{0.664 f_o}{\left(Re_{th} \tan \alpha\right)^{1/2}} \int_1^{A_e/A_{th}} f_1 f_2 \, d\left(\frac{A}{A_{th}}\right) \tag{7}$$

where

$$f_o = \gamma \left(\frac{\frac{\mu_w}{\mu_{th}} \frac{\rho_{th}}{\rho_o} \sqrt{\frac{T_{th}}{T_o}}}{2 \frac{T_w}{T_o}} \right)^{1/2}$$

$$f_1 = \left(\sqrt{\frac{A}{A_{th}}} - 1 \right)^{-1/2}$$

$$f_2 = M^{1.5} \left(\frac{T}{T_o} \right)^{\frac{5\gamma - 3}{4(\gamma - 1)}}$$

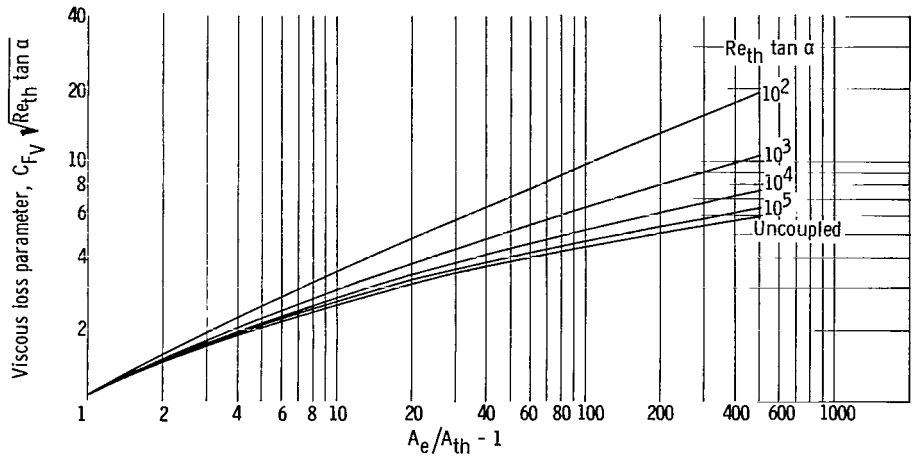

Figure 2. - Viscous losses as given by laminar-flow flat-plate theory. Stagnation temperature, 530° R; wall- to stagnation-temperature ratio, 1.0.

In order to evaluate C_{F_v} it is necessary to specify the wall temperature and the nozzle stagnation conditions. The local flow conditions throughout the nozzle can be determined approximately in terms of the stagnation conditions from one-dimensional isentropic-flow relations. The local stream conditions, M and T/T_o, in the factor f_2 may be evaluated at either the geometric nozzle area ratio (uncoupled case) or an effective nozzle area ratio (coupled case). The coupled case attempts to include the influence of the boundary layer on the local stream properties in terms of a reduced nozzle area ratio. For the coupled case, the effective nozzle area ratio is defined in terms of the displacement thickness δ^* by

$$\left(\frac{A}{A_{th}}\right)_{eff} = \left(1 - \frac{\delta^*}{r}\right)^2 \frac{A}{A_{th}} \tag{8}$$

where δ^*/r is determined as outlined in appendix B.

Figure 2 presents the results for the numerical integration of equation (7) for hydrogen ($\gamma = 1.4$) at cold-flow conditions ($T_o = 530^o$ R, $T_w/T_o \approx 1.0$) for both the uncoupled and coupled cases. As the value of the parameter ($Re_{th}\tan\alpha$) decreases, the loss in thrust coefficient due to viscous effects increases.

Figure 3 presents the loss in thrust coefficient for a nozzle with a divergence angle of 20^o for the coupled solution. The increasing losses resulting from increasing area ratio and decreasing throat Reynolds number are evident.

Figure 4 presents the net thrust coefficient, including the viscous losses, as given in figure 3, for a nozzle divergence angle of 20^o. This divergence angle was used because preliminary calculations showed that, for a given nozzle area ratio and throat Reynolds

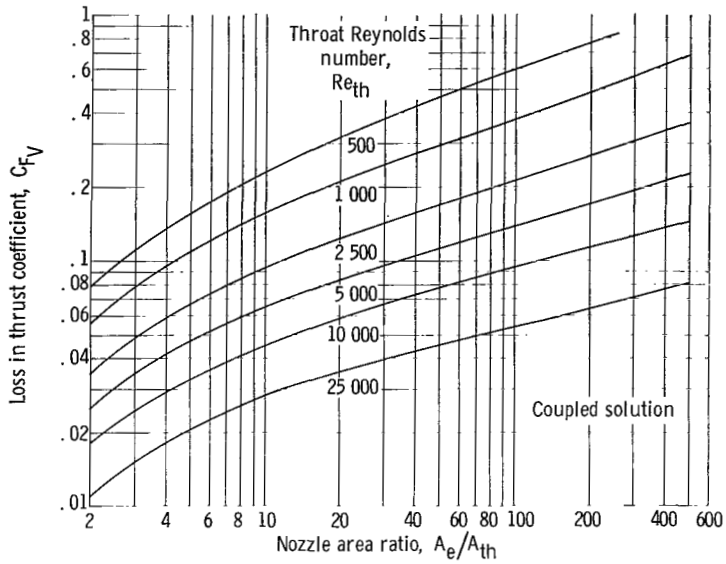

Figure 3. - Loss in thrust coefficient due to viscous effects as given by laminar-flow flat-plate theory. Stagnation temperature, 530° R; wall- to stagnation-temperature ratio, 1.0; nozzle divergence angle, 20°.

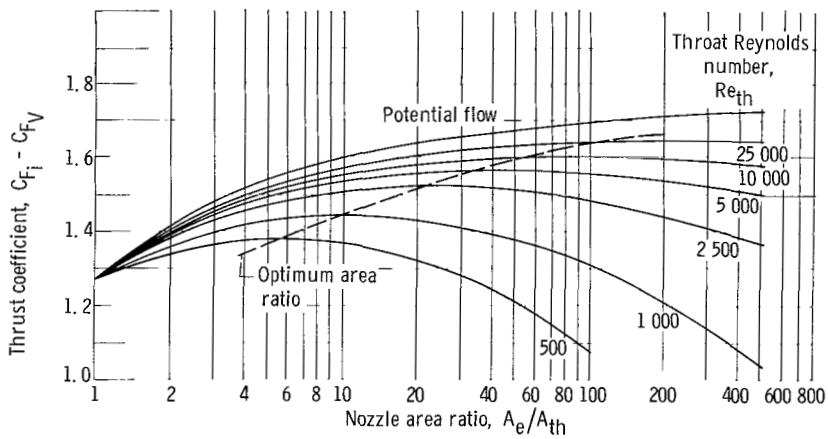

Figure 4. - Thrust coefficient including viscous losses as given by laminar-flow flat-plate theory. Stagnation temperature, 530° R; wall- to stagnation-temperature ratio, 1.0; nozzle divergence angle, 20°.

number, the thrust coefficient is not greatly affected by changes in the divergence angle for $15^{\circ} < \alpha < 25^{\circ}$. The optimization of the thrust coefficient with area ratio, as shown in figure 4, occurs because the gains due to the increased area ratio are less than the additional viscous losses imposed by the increased surface area. The significant loss in thrust coefficient and the low optimum area ratios at low throat Reynolds numbers are important factors that must be considered for the application of low-thrust devices.

EXPERIMENTAL APPARATUS

The objective of this experimental program was to obtain performance data on a

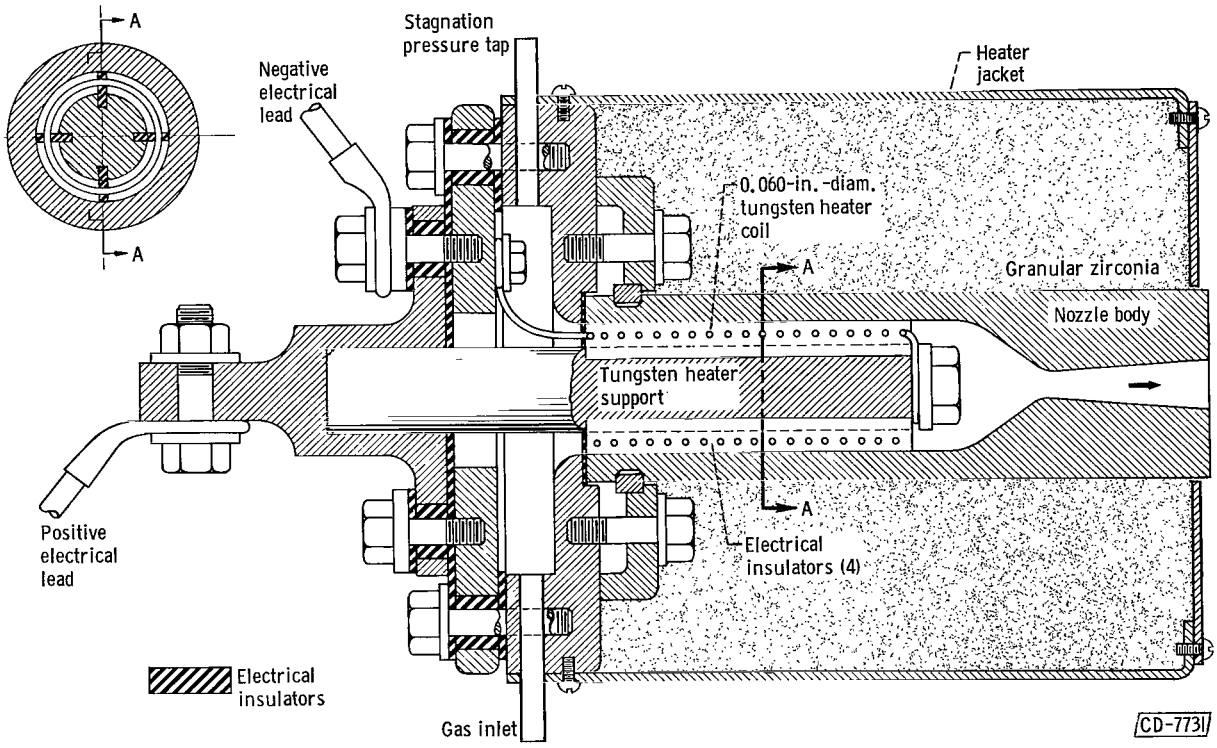

Figure 5. - Wire coil resistance-heated thrustor.

resistojet with hydrogen as the propellant at low-thrust levels for various nozzle area ratios and throat Reynolds numbers. The resistojet is reasonably well suited for providing the necessary data in that its operating characteristics are inherently stable and reliable over a wide range of operating conditions. A specified operating point can be set and maintained until equilibrium conditions are achieved.

Thrustor Description

The performance of resistance-heated hydrogen thrustors has been under investigation for a number of years. Results of some of these studies are presented in references 7, 10, and 11. Figure 5 illustrates the thrustor design used in reference 7 and in the present investigation. Basically, the design consists of a tungsten-wire coil heater inserted into a nozzle body. The outer surface of the nozzle body is surrounded by a thick layer of insulation to minimize heat losses. The propellant is heated while passing directly over the heater coil and is expelled through the nozzle. Table I indicates the seven different nozzle geometries used during the experimental program to provide the desired variations in nozzle area ratio and throat diameter. Two basic thrustor designs were used that differed only in size and method of supporting the heater coil. These two

TABLE I. - NOZZLE GEOMETRIES AND COLD-FLOW DATA

Unit designation (a)	Nozzle area ratio, A_e/A_{th}	Nozzle throat flow area, A_{th}, sq in.	Isentropic thrust coefficient, C_{F_i}	Propellant flow rate, $\dot{w}$, lb/sec	Measured total pressure, P_m, psia	Measured thrust, F_m, lb	Measured thrust coefficient, C_{F_m}	Difference between calculated isentropic and measured thrust coefficient, C_{F_ℓ}	Throat Reynolds number, Re_{th}
3W25	25	3.63×10^{-3}	1.652	2.5×10^{-4}	11.5	60.9×10^{-3}	1.455	0.197	11 000
				1.0	4.79	22.9	1.318	.334	4 400
				.5	2.44	10.57	1.192	.460	2 200
3BN50	50	3.84×10^{-3}	1.677	2.5×10^{-4}	11.18	61.9×10^{-3}	1.442	0.235	10 700
				1.0	4.60	23.9	1.353	.324	4 280
				.5	2.30	10.78	1.222	.455	2 140
3BN75	75	3.63×10^{-3}	1.691	2.5×10^{-4}	11.73	61.2×10^{-3}	1.438	0.253	11 000
				1.0	4.78	23.1	1.331	.360	4 400
				.5	2.48	10.58	1.175	.516	2 200
3BN100	100	4.07×10^{-3}	1.696	2.5×10^{-4}	10.3	59.8×10^{-3}	1.425	0.271	10 420
				1.0	4.39	22.05	1.234	.462	4 170
				.5	2.28	10.02	1.081	.615	2 085
4BN100	100	4.65×10^{-3}	1.696	2.5×10^{-4}	8.7	61.7×10^{-3}	1.526	0.170	9 730
				1.0	3.6	22.7	1.355	.341	3 890
				.5	1.9	10.46	1.182	.514	1 945
4BN40	40	11.90×10^{-3}	1.670	2.5×10^{-4}	3.55	59.8×10^{-3}	1.415	0.255	6 080
				1.0	1.50	21.85	1.224	.446	2 430
				.5	.80	10.02	1.052	.618	1 215
3BN150	150	1.32×10^{-3}	1.705	2.5×10^{-4}	31.05	59.8×10^{-3}	1.456	0.249	18 330
				1.0	12.62	22.5	1.350	.355	7 320
				.5	6.48	10.14	1.188	.517	3 665

[a] First digit: 3 has 1/2-in.-diam heater coil and boron nitride heater supports, while 4 has 1-in.-diam heater coil and tungsten heater supports; letters W and BN indicate tungsten or boron nitride nozzle body; last digits indicate nozzle area ratio.

thrustors are identified in table I by the first digit of the unit designation. The number 3 refers to a unit with a 1/2-inch-diameter heater coil with heater supports made of boron nitride. The number 4 corresponds to a 1-inch-diameter heater coil with heater supports made of tungsten. The letters W and BN refer to tungsten or boron nitride nozzle bodies, respectively. Only the 3W25 unit has a tungsten nozzle body. All other nozzle bodies were made of boron nitride to simplify fabrication. The boron nitride nozzle bodies performed satisfactorily for the comparatively short runs and moderate temperatures required to obtain the necessary performance data. The remaining digits indicate the nozzle area ratio.

Range of Test Parameters

Data were obtained on each of the seven different nozzles at propellant flow rates of 0.5×10^{-4}, 1.0×10^{-4}, and 2.5×10^{-4} pound per second. For each of these propellant flow rates, specific power (input electrical power/propellant flow rate) values of 0, 0.5×10^{4}, 1.0×10^{4}, and 1.5×10^{4} kilowatts per pound per second were used except for the lowest propellant flow rate of 0.5×10^{-4} pound per second. At this flow rate, a single specific power point of approximately 1.2×10^{4} kilowatts per pound per second was used corresponding to the minimum current output of the power supply for the heater coils used. No higher specific power points were attempted because of the marginal thrustor cooling at this low flow rate.

The maximum specific power value was limited to 1.5×10^{4} kilowatts per pound per second to minimize the component problems that are encountered at the higher propellant temperatures. Each specific power point was held for a period of time in excess of 15 minutes, during which time the measured stagnation pressure was monitored to assure that equilibrium conditions had been achieved.

Research Facility and Instrumentation

The experimental program was conducted in one of the large vacuum tanks at the Lewis Research Center. This facility (described in detail in ref. 12) has a diameter of 15 feet and a length of 63 feet. Exhaust pumping speed capabilities of 12 000 cubic feet per minute provided ambient pressures below 0.3 millimeter of mercury for all propellant flow rates. The low ambient pressures were more than sufficient to ensure complete expansion for all the nozzle area ratios studied. Electrical power was supplied by a commercial solid-state conversion d-c power supply. Gaseous hydrogen was supplied from a bank of four commercial hydrogen bottles.

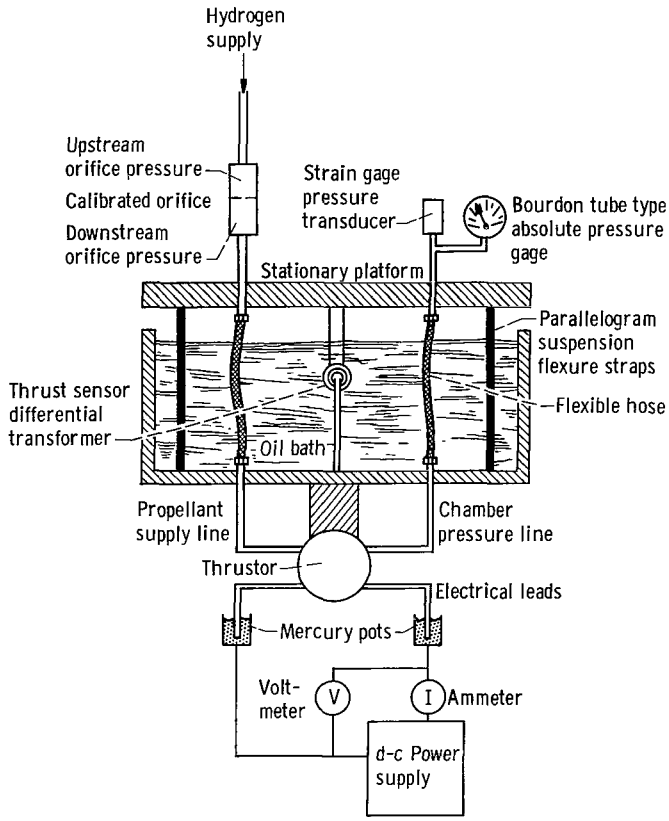

Figure 6. - Schematic drawing of thrust stand and instrumentation.

A schematic drawing of the thrustor mounting and system instrumentation is shown in figure 6. The propellant flow rate was metered by a calibrated choked orifice with strain-gage pressure transducers to measure orifice upstream and downstream pressures. Thrustor chamber pressure was measured with a Bourdon tube-type absolute-pressure gage and a strain-gage pressure transducer. Voltage and current measurements were made with conventional instrumentation. Thrust measurements were made with a four-point suspension-platform-type thrust stand (ref. 13). A differential transformer immersed in an oil bath, to maintain a constant-temperature environment, was used as the thrust-sensing element.

The overall measurement accuracy of the data is as follows: chamber pressure and propellant flow rate measurements are accurate to within ±2 percent. Thrust measurements as determined by weight calibration before each test run under vacuum conditions are accurate to within ±1 millipound. The overall accuracy of the measured thrust coefficient is estimated to be approximately ±10 percent at the low-thrust levels and ±3 percent at the high-thrust levels.

DATA REDUCTION

The measured data, along with other computed values, are presented in tables I and II for each of the seven different nozzle configurations. Table I (p. 8) presents the cold-flow data (obtained without heat addition) and table II presents the hot-flow data (obtained with heat addition to the propellant).

The measured thrust coefficient and the corresponding loss in thrust coefficient are calculated as

$$C_F = \frac{F_m}{P_m A_{th}} \tag{9}$$

TABLE II. - HOT-FLOW DATA

Unit designation (a)	Nozzle area ratio, A_e/A_{th}	Nozzle throat flow area, A_{th}, sq in.	Isentropic thrust coefficient, C_{F_i}	Propellant flow rate, $\dot{w}$, lb/sec	Measured total pressure, P_m, psia	Measured thrust, F_m, lb	Measured thrust coefficient, C_{F_m}	Difference between calculated isentropic and measured thrust coefficient, C_{F_ℓ}	Throat Reynolds number, Re_{th}
3W25	25	3.63×10^{-3}	1.652	2.5×10^{-4}	21.5	114.5×10^{-3}	1.468	0.184	4770
				2.5	23.4	124.2	1.463	.189	4270
				1.0	9.4	43.4	1.280	.372	1785
				1.0	10.4	47.8	1.267	.385	1565
				1.0	9.0	42.7	1.308	.344	1895
				1.0	10.35	48.9	1.300	.352	1575
				1.0	10.5	48.7	1.278	.374	1550
				1.0	11.3	51.6	1.259	.393	1400
				.5	4.9	18.7	1.051	.601	867
				.5	5.0	19.6	1.080	.572	844
				.5	5.1	19.8	1.070	.582	823
				.5	4.9	18.05	1.014	.638	867
3BN50	50	3.84×10^{-3}	1.677	2.5×10^{-4}	20.6	113.0×10^{-3}	1.430	0.247	4740
				2.5	25.3	137.0	1.410	.267	3610
				2.5	28.5	153.0	1.398	.279	3070
				1.0	8.75	42.3	1.260	.417	1820
				1.0	10.3	48.9	1.235	.442	1465
				1.0	11.05	51.8	1.220	.457	1330
				1.0	11.75	53.8	1.193	.484	1225
				.5	4.4	18.05	1.068	.609	903
3BN75	75	3.63×10^{-3}	1.691	2.5×10^{-4}	22.0	118.5×10^{-3}	1.485	0.206	4750
				2.5	25.7	136.5	1.462	.229	3890
				2.5	28.9	153.0	1.458	.233	3300
				1.0	9.4	46.1	1.350	.341	1780
				1.0	11.0	50.3	1.261	.430	1445
				1.0	11.8	52.7	1.230	.461	1330
				.5	4.9	18.5	1.040	.651	890
3BN100	100	4.07×10^{-3}	1.696	2.5×10^{-4}	21.4	123.6×10^{-3}	1.420	0.276	3940
				2.5	24.8	142.6	1.413	.283	3220
				2.5	25.9	145.5	1.381	.315	3050
				2.5	20.5	121.3	1.455	.241	4170
				2.5	24.9	141.4	1.396	.300	3200
				1.0	8.4	41.9	1.225	.471	1755
				1.0	9.82	50.8	1.272	.424	1430
				1.0	11.2	54.2	1.190	.506	1195
				1.0	9.9	47.9	1.190	.506	1405
				1.0	10.15	53.3	1.173	.523	1205
				.5	4.35	17.43	.985	.711	880
				.5	4.40	18.05	1.010	.686	867

[a]First digit: 3 has 1/2-in.-diam heater coil and boron nitride heater supports, while 4 has 1-in.-diam heater coil and tungsten heater supports; letters W and BN indicate tungsten or boron nitride nozzle body; last digits indicate nozzle area ratio.

TABLE II. - Concluded. HOT-FLOW DATA

Unit designation [a]	Nozzle area ratio, A_e/A_{th}	Nozzle throat flow area, A_{th}, sq in.	Isentropic thrust coefficient, C_{F_i}	Propellant flow rate, $\dot{w}$, lb/sec	Measured total pressure, P_m, psia	Measured thrust, F_m, lb	Measured thrust coefficient, C_{F_m}	Difference between calculated isentropic and measured thrust coefficient, C_{F_ℓ}	Throat Reynolds number, Re_{th}
4BN100	100	4.65×10^{-3}	1.676	2.5×10^{-4}	15.9	113.4×10^{-3}	1.534	0.162	4310
				2.5	21.1	147.0	1.497	.199	2970
				2.5	23.3	160.4	1.480	.216	2610
				1.0	8.5	48.7	1.232	.464	1235
				1.0	7.9	48.1	1.310	.386	1370
				1.0	7.2	45.2	1.350	.346	1545
				1.0	9.1	54.4	1.285	.411	1128
				.5	3.4	18.3	1.157	.539	895
				.5	3.8	19.6	1.110	.586	773
4BN40	40	11.90×10^{-3}	1.670	2.5×10^{-4}	6.6	110.7×10^{-3}	1.408	0.262	2650
				2.5	8.35	135.2	1.360	.310	1945
				2.5	9.6	154.0	1.348	.322	1615
				1.0	2.70	39.1	1.217	.453	1095
				1.0	3.35	46.6	1.170	.553	838
				1.0	3.90	52.3	1.127	.543	680
				.5	1.70	18.54	.917	.753	443
				.5	1.78	18.95	.895	.775	425
3BN150	150	1.32×10^{-3}	1.705	2.5×10^{-4}	59.4	118.5×10^{-3}	1.512	0.193	7740
				2.5	59.05	116.8	1.496	.209	7800
				2.5	73.8	145.4	1.491	.214	5780
				2.5	78.4	158.4	1.532	.173	5360
				1.0	24.4	43.0	1.335	.370	3050
				1.0	28.6	48.5	1.285	.420	2460
				1.0	31.85	53.0	1.260	.445	2140
				.5	13.0	17.86	1.041	.664	1445

[a] First digit: 3 has 1/2-in. -diam heater coil and boron nitride heater supports, while 4 has 1-in. -diam heater coil and tungsten heater supports; letters W and BN indicate tungsten or boron nitride nozzle body; last digits indicate nozzle area ratio.

$$C_{F_\ell} = C_{F_i} - C_{F_m} \tag{10}$$

The throat Reynolds number is defined as

$$Re_{th} = \frac{\dot{w}}{A_{th}} \frac{d_{th}}{\mu_{th}} \tag{11}$$

Since the propellant temperature was not measured (except at the cold-flow conditions), the viscosity for the hot-flow data could not be explicitly evaluated. Therefore the following approximate method was used to determine the throat Reynolds numbers.

For the cold-flow data, the viscosity was evaluated at the throat temperature corresponding to an isentropic process from the known stagnation temperature of 530° R. For the hot data, the throat Reynolds number ratio ($Re_{th, cold}/Re_{th, hot}$) for the same nozzle throat diameter and the same propellant flow rate is given by

$$\frac{Re_{th, hot}}{Re_{th, cold}} = \frac{\mu_{th, cold}}{\mu_{th, hot}} \tag{12}$$

For the temperature range covered, an adequate expression for the viscosity of hydrogen (fitted to the data of ref. 3) is $\mu \propto T^{2/3}$. Equation (12) can then be expressed as

$$\frac{Re_{th, hot}}{Re_{th, cold}} = \left(\frac{T_{th, cold}}{T_{th, hot}}\right)^{2/3} \tag{13}$$

For a one-dimensional isentropic process, the temperature at the nozzle throat is proportional to $(P_{th}A_{th}/\dot{w})^2$. For conditions in which the nozzle throat area and propellant flow rate are constant, the temperature ratio in equation (13) is then given by

$$\frac{T_{th, cold}}{T_{th, hot}} = \left(\frac{P_{th, cold}}{P_{th, hot}}\right)^2 \tag{14}$$

If it is assumed that the pressure at the nozzle throat and the measured chamber pressure are similarly related for conditions of both hot and cold flow as

$$\left(\frac{P_{th}}{P_m}\right)_{cold} \approx \left(\frac{P_{th}}{P_m}\right)_{hot}$$

the ratio of the cold to the hot throat Reynolds number can be approximated by

$$\frac{Re_{th,\,hot}}{Re_{th,\,cold}} \approx \left(\frac{P_{m,\,cold}}{P_{m,\,hot}}\right)^{4/3} \tag{15}$$

Although this approximate procedure for estimating the propellant temperature may introduce inaccuracies, the resulting error is considered to be within the experimental accuracies of the other parameters.

EXPERIMENTAL RESULTS

The experimental data are suitable for the determination of thrustor performance but they are not suitable for a precise interpretation of the nature or the mechanism of the nozzle losses. This statement is especially applicable to the hot data, which includes both viscous and heat-transfer effects, that cannot be separated from each other. The data are useful, however, to identify correlating parameters for analytically predicting overall performance.

Figure 7 presents the thrust coefficient for the cold and the hot data for the 3W25 nozzle. The trends exhibited by these data are typical of all the other nozzles. The decreasing thrust coefficient with decreasing throat Reynolds number is consistent with the predictions of the laminar-flat-plate analysis, but the magnitude of the measured thrust coefficients is much less. This was not unexpected and indicates that the conical nozzle losses are much higher than the calculated laminar-flat-plate losses. The magnitude of the measured thrust coefficients at the low throat Reynolds numbers is also significant. The measured thrust coefficient decreases from a value of approximately 1.45 at $Re_{th} \approx 10\,000$ to a value of approximately 1.05 at $Re_{th} \approx 850$. This latter value is less than the calculated isentropic thrust coefficient (1.27) for a choked orifice.

In figure 7, the hot-flow thrust coefficients are higher than the cold-flow values at a given throat Reynolds number. If equation (7) is used as a guide to estimate the difference between the hot and cold data, the experimental trend is contrary to that predicted by the analysis. The only parameter in equation (7) that changes as a result of the

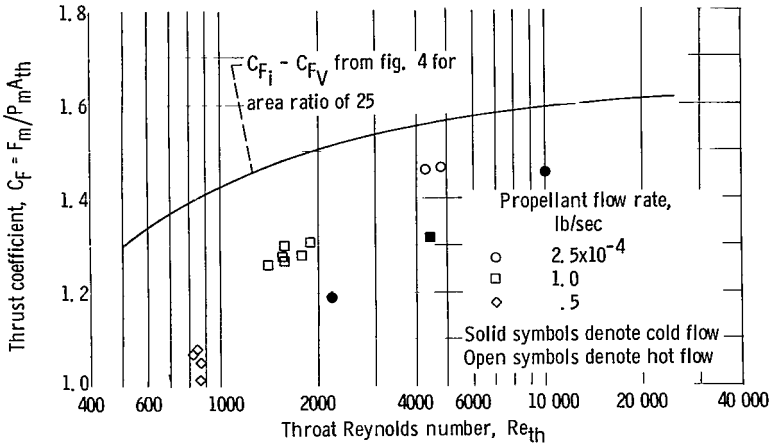

Figure 7. - Typical comparison of hot and cold thrust coefficients. Unit designation, 3W25.

differences between the hot and cold operating conditions is the factor f_o, which depends on the wall temperature. For cold flow, the expansion process is essentially adiabatic, and therefore $T_w/T_o \approx 1.0$. For hot flow where cooling of the nozzle walls occurs by radiation, $T_w/T_o < 1.0$. As T_w/T_o decreases, the loss in thrust coefficient, as given by equation (7) (including viscosity effects), increases and correspondingly the thrust coefficient for the hot-flow data at a given throat Reynolds number should be less than that for the cold data. The experimental data therefore indicate that the throat Reynolds number based on the local stream temperature is not a good correlating parameter both for the hot- and cold-flow data.

Even though the free-stream throat Reynolds number would not correlate both the hot and cold data, it seemed probable that a suitable correlation could be developed for the loss in thrust coefficient if the throat Reynolds number were based on an appropriate reference temperature. The nozzle-wall temperature was found to be an acceptable choice. The throat Reynolds number based on the wall temperature is given by

$$Re_{th,w} \equiv \left(\frac{\rho_w u d}{\mu_w}\right)_{th} \tag{16}$$

In terms of the previous throat Reynolds number, equation (16) becomes

$$Re_{th,w} = Re_{th}\left(\frac{\rho_w}{\rho}\frac{\mu}{\mu_w}\right)_{th} \tag{17}$$

For the conventional boundary-layer assumption of zero radial pressure gradient and a viscosity-temperature relation for hydrogen of $\mu \propto T^{2/3}$, $Re_{th,w}$ is given by

$$Re_{th,w} = Re_{th}\left(\frac{T}{T_w}\right)_{th}^{5/3} \tag{18}$$

For the cold-flow data, the nozzle-wall temperature can be approximated by the adiabatic wall temperature. Thus, for a laminar recovery factor of 0.84,

$$\left(\frac{T}{T_w}\right)_{th,\,cold} = 0.857 \tag{19}$$

For the hot data, an estimate of $(T/T_w)_{th}$ is not as straightforward. Optical pyrometer measurements indicated that the nozzle-wall temperature for similar operating conditions was of the order of $0.50 < T_w/T_E < 0.66$, where T_E is the ideal temperature the propellant would attain in the heater chamber for a heating efficiency of unity (i.e., if all the input electrical power were converted to thermal energy). If T_E is introduced,

$$\left(\frac{T}{T_w}\right)_{th,\,hot} = \frac{\dfrac{T_{th}}{T_E}}{\dfrac{T_{w,\,th}}{T_E}} \tag{20}$$

If the value of T_{th}/T_E is taken as the one-dimensional isentropic value of 0.833 and $T_{w,\,th}/T_E$ is approximated as $T_{w,\,th}/T_E \approx T_w/T_E \approx 0.6$, an estimate for $(T/T_w)_{th,\,hot}$ is

$$\left(\frac{T}{T_w}\right)_{th,\,hot} = \frac{0.833}{0.60} = 1.388 \tag{21}$$

Although a constant value of $(T/T_w)_{th,\,hot}$ is unlikely for the complete range of operating conditions covered herein, a more accurate value could not be obtained in this investigation.

Figure 8 is a comparison of the hot and cold losses in thrust coefficient in terms of $Re_{th,w}$ for each of the seven different nozzles. The data indicate, in general, that, at the high propellant flow rates where the heat-transfer losses and thermal-boundary layer are small, the hot and cold loss in thrust coefficient are of the same magnitude. As the propellant flow rate decreases, the losses for the hot data tend to increase over that of the cold-flow data at the same value of $Re_{th,w}$.

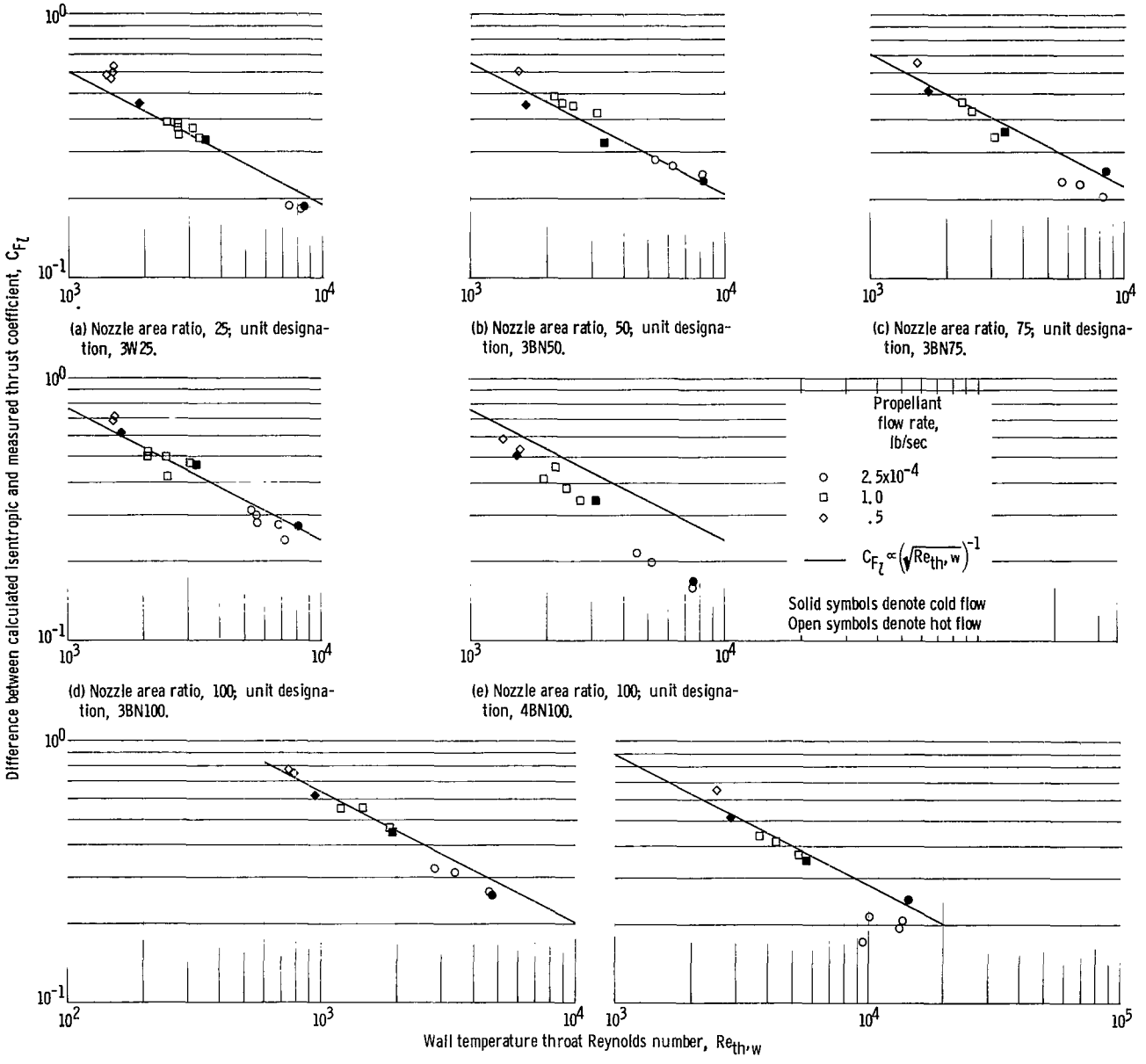

(a) Nozzle area ratio, 25; unit designation, 3W25.

(b) Nozzle area ratio, 50; unit designation, 3BN50.

(c) Nozzle area ratio, 75; unit designation, 3BN75.

(d) Nozzle area ratio, 100; unit designation, 3BN100.

(e) Nozzle area ratio, 100; unit designation, 4BN100.

(f) Nozzle area ratio, 40; unit designation, 4BN40.

(g) Nozzle area ratio, 150; unit designation, 3BN150.

Figure 8. - Comparison of hot and cold data in terms of wall temperature throat Reynolds number.

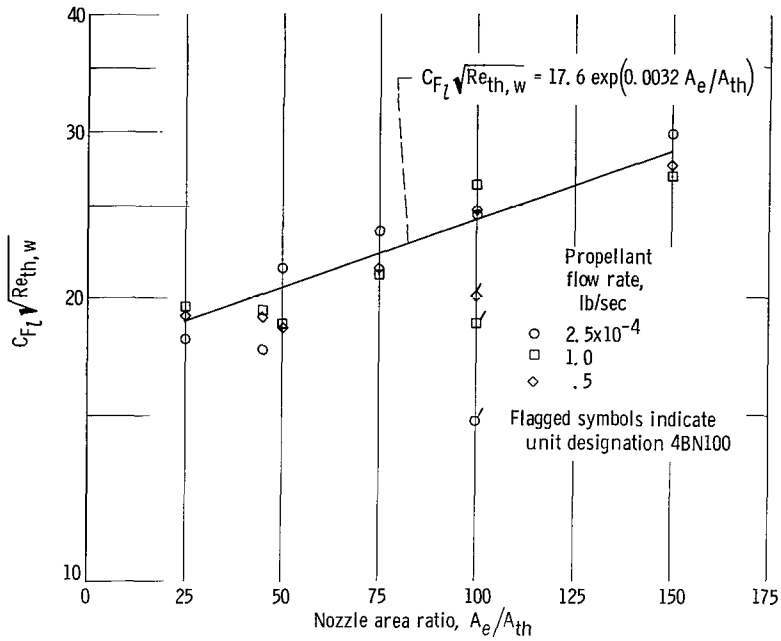

Figure 9. - Correlation of loss in thrust coefficient for cold-flow data.

The curves shown in figure 8 have the functional form $C_{F_v} \propto (Re_{th,w})^{-1/2}$ and are a consistent and reasonable approximation of the data, except for the 4BN100 nozzle. The data obtained with the 4BN100 nozzle were much different from the data obtained with the 3BN100 nozzle. In addition, the slope of the line to fit the 4BN100 nozzle data was not consistent with the data from all the other nozzles. No explanation can be given for this difference.

All the data (except that for the 4BN100 nozzle) presented in figure 8 exhibited a consistent trend of increasing losses with increasing nozzle area ratio. The area-ratio correlation can best be shown in terms of the cold-flow data as presented in figure 9. Based on a straight-line correlation of the data, the final relation for the loss in thrust coefficient is given by

$$C_{F_\ell} = \frac{17.6 \exp\left(0.0032 \dfrac{A_e}{A_{th}}\right)}{(Re_{th,w})^{1/2}}$$

The effectiveness of this correlation to estimate the thrust coefficient for both cold- and hot-flow conditions for the area ratios investigated is shown in figure 10. The data lie in a ±5-percent band, except for the data from the 4BN100 nozzle and the data at the lowest propellant flow rate. It is believed that the reason the data at the lowest propellant flow rate deviate from the correlation is that the heat-transfer losses become more

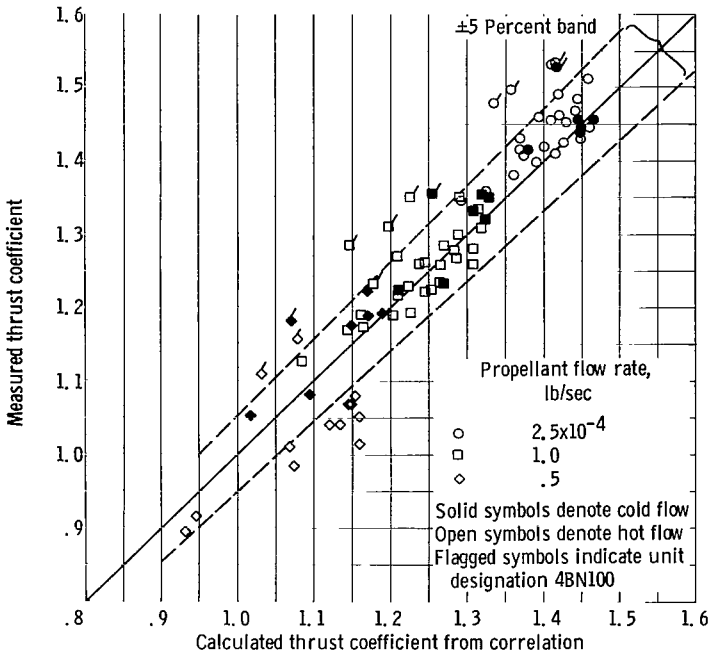

Figure 10. - Comparison of experimental thrust coefficients with values calculated from correlation.

important at low throat Reynolds numbers. However, these data at the low propellant flow rates should not be considered as general but rather as characteristic of the radiation-cooled thrustor used in this study. Heat-transfer losses are governed by design considerations. Other nozzle-cooling methods, sizes, and materials could yield different results.

The approximations made to obtain the final correlation of the data may not be suitable for other ranges of propellant flow rates and specific power levels than those investigated herein. For example, it has been assumed that $T_w/T_E = 0.6$ for the hot data and that $T_w/T_E = 1.0$ for the cold-flow test data. This temperature ratio, of course, must vary continuously with the propellant temperature. Furthermore, the nozzle-wall temperature has an axial variation and is not constant as was assumed. Additional research is required to refine the correlation and to understand better the various mechanisms contributing to the losses in low-thrust-level nozzles.

CONCLUSIONS

The following conclusions regarding the performance losses of nozzles at low-thrust levels have been drawn from the experimental data:

1. Nozzle losses can seriously degrade the thrust coefficient of nozzles with low throat Reynolds numbers to values much below those calculated for an isentropic expansion process. In fact, thrust coefficients were measured that were less than the calculated thrust coefficient for isentropic flow through a choked orifice.

2. The measured nozzle losses are significantly greater than the viscous losses calculated from the skin friction relation for laminar flow over a flat plate. The trends, however, in terms of increasing losses with decreasing throat Reynolds numbers are similar.

3. A qualitative correlation of the loss in thrust coefficient for both the hot and cold data was obtained in terms of the nozzle area ratio and throat Reynolds number in which the temperature-dependent properties (density and viscosity) are evaluated at the nozzle wall temperature.

Lewis Research Center,
National Aeronautics and Space Administration,
Cleveland, Ohio, July 26, 1965.

APPENDIX A

SYMBOLS

A	nozzle flow area
A/A_{th}	geometric nozzle area ratio
$(A/A_{th})_{eff}$	effective nozzle area ratio
C	factor of proportionality in eq. (B7), $\mu_w/\mu = C(T_w/T)$
C_F	thrust coefficient, F/P_oA_{th}
C_{F_ℓ}	difference between calculated isentropic thrust coefficient and measured thrust coefficient
C_{F_v}	loss in thrust coefficient due to boundary-layer viscous losses, F_v/P_oA_{th}
d	nozzle diameter
F	thrust
F_ℓ	loss in thrust due to nozzle losses
F_v	loss in thrust due to viscous drag on nozzle surface
g	gravity acceleration
M	Mach number
P	total pressure
p	pressure
Re	Reynolds number
r	nozzle radius
S	nozzle surface
s	distance along nozzle surface
T	temperature
T_E	ideal temperature attained by propellant for heating efficiency of unity
u	fluid velocity
$\dot{w}$	propellant flow rate
x	axial distance along nozzle
α	nozzle divergence angle
γ	specific heat ratio
δ^*	displacement thickness
λ	nozzle angle divergence coefficient, $\lambda = (1 + \cos \alpha)/2$
μ	fluid viscosity
ρ	fluid density
τ	shear stress

Subscripts:

e	nozzle-exit conditions
ht	heat-transfer effects
i	isentropic conditions
m	experimentally measured values
o	stagnation conditions upstream of nozzle throat
th	throat conditions
v	viscous effects
w	wall conditions
x	axial component

APPENDIX B

CONICAL NOZZLE VISCOUS LOSSES

It will be assumed in the following development that (1) the important viscous losses take place in the supersonic portion of the nozzle, (2) the boundary layer begins at the nozzle throat, (3) the nozzle is an isothermal surface, and (4) the local flow conditions can be obtained in terms of the stagnation conditions from one-dimensional isentropic-flow relations. The divergent portion of a conical nozzle with pertinent coordinates is shown in figure 1 (p. 3).

The loss in thrust due to the axial component of the viscous drag is given by the surface integral of the local shear stress over the nozzle surface:

$$F_v = \int_S 2\pi\tau r \cos\alpha \, ds \tag{B1}$$

For purposes of calculation, it is desirable to express equation (B1) in terms of the geometric nozzle area ratio A/A_{th}. The linear coordinates are related to the nozzle area ratio as follows:

$$\frac{x}{d_{th}} = \frac{\sqrt{\frac{A}{A_{th}}} - 1}{2 \tan\alpha} \tag{B2}$$

$$dx = \frac{d_{th}}{4\sqrt{\frac{A}{A_{th}}} \tan\alpha} d\left(\frac{A}{A_{th}}\right) = ds \cos\alpha \tag{B3}$$

Equation (B1) may now be written in the form

$$F_v = \int_1^{A_e/A_{th}} \frac{\tau A_{th}}{\tan\alpha} d\left(\frac{A}{A_{th}}\right) \tag{B4}$$

The loss in thrust can be expressed in terms of a loss in thrust coefficient C_{F_v} by

$$C_{F_v} \equiv \frac{F_v}{P_o A_{th}} = \frac{1}{P_o \tan \alpha} \int_1^{A_e/A_{th}} \tau d\left(\frac{A}{A_{th}}\right) \tag{B5}$$

The loss in thrust coefficient can be computed by substituting into equation (B5) the appropriate expression for the local shear stress τ and then performing the indicated integration. Unfortunately no useful relations for the laminar shear stress on a nozzle surface are known. However, the skin friction relation for laminar flow over an isothermal flat plate provides a simple initial approximation for comparison with experiment. This expression, as given in reference 9, is

$$\frac{\tau}{\frac{1}{2}\rho u^2} = 0.664\, C^{0.5} \left(\frac{\rho u x}{\mu}\right)^{-0.5} \tag{B6}$$

The constant C relates the viscosity and temperature at the wall and free-stream conditions:

$$\frac{\mu_w}{\mu} = C\left(\frac{T_w}{T}\right) \tag{B7}$$

The local length Reynolds number in equation (B6) can be expressed in terms of the nozzle throat Reynolds number Re_{th} as follows:

$$\frac{\rho u x}{\mu} = Re_{th} \frac{\rho}{\rho_{th}} \frac{u}{u_{th}} \frac{x}{d_{th}} \frac{\mu_{th}}{\mu} \tag{B8}$$

By suitable substitution of the one-dimensional isentropic-flow relations and equation (B2) into equation (B8), the local length Reynolds number can be written as

$$\frac{\rho u x}{\mu} = \left(\frac{\frac{\mu_{th}}{\mu_o}}{2\frac{\rho_{th}}{\rho_o}\sqrt{\frac{T_{th}}{T_o}}}\right) Re_{th} M \left(\frac{T}{T_o}\right)^{\frac{\gamma+1}{2(\gamma-1)}} \left(\frac{\sqrt{\frac{A}{A_{th}}} - 1}{\tan \alpha}\right) \frac{\mu_o}{\mu} \tag{B9}$$

For a perfect gas, $\frac{1}{2}\rho u^2$ is given by

$$\frac{1}{2}\rho u^2 = \frac{\gamma}{2} P_o M^2 \left(\frac{T}{T_o}\right)^{\frac{\gamma}{\gamma-1}} \tag{B10}$$

Substituting equations (B7), (B9), and (B10) into equation (B6), and the resulting expression for the shear stress into equation (B5) yields

$$C_{F_v} = \frac{0.664\, f_o}{(Re_{th} \tan \alpha)^{1/2}} \int_1^{A_e/A_{th}} f_1 f_2 \, d\left(\frac{A}{A_{th}}\right) \tag{B11}$$

where

$$f_o = \gamma \left(\frac{\frac{\mu_w}{\mu_{th}} \frac{\rho_{th}}{\rho_o} \sqrt{\frac{T_{th}}{T_o}}}{2 \frac{T_w}{T_o}} \right)^{1/2}$$

$$f_1 = \left(\sqrt{\frac{A}{A_{th}}} - 1 \right)^{-1/2}$$

$$f_2 = M^{1.5} \left(\frac{T}{T_o}\right)^{\frac{5\gamma-3}{4(\gamma-1)}}$$

The local stream properties M and T/T_o in the parameter f_2 are evaluated from one-dimensional isentropic relations for the local geometric nozzle area ratio (uncoupled case) or at an effective nozzle area ratio (coupled solution), which includes the influence of the boundary-layer growth on the free-stream conditions.

For the coupled solution, the effective nozzle area ratio is defined in terms of the boundary-layer displacement thickness and geometric nozzle area ratio by

$$\left(\frac{A}{A_{th}}\right)_{eff} = \frac{A}{A_{th}} \left(1 - \frac{\delta^*}{r}\right)^2 \tag{B12}$$

where

$$\frac{\delta^*}{r} = \frac{\delta^*}{x}\,\frac{x}{r_{th}}\,\frac{r_{th}}{r} = \frac{\delta^*}{x}\,\frac{\sqrt{\frac{A}{A_{th}}} - 1}{\tan\alpha\sqrt{\frac{A}{A_{th}}}} \tag{B13}$$

For laminar flow over a flat plate with constant wall temperature, δ^*/x may be derived from reference 9 as

$$\frac{\delta^*}{x} = C^{1/2}\left(\frac{\rho u x}{\mu}\right)^{-1/2}\left[1.73 + 1.11(\gamma - 1)M^2\right] \tag{B14}$$

where C and the local length Reynolds number are given by equations (B7) and (B9). Hence, δ^*/r may be expressed as

$$\frac{\delta^*}{r} = \frac{g_o g_1 g_2}{(Re_{th}\tan\alpha)^{1/2}} \tag{B15}$$

where

$$g_o = \left(\frac{2\,\frac{\mu_w}{\mu_{th}}\,\frac{\rho_{th}}{\rho_o}\sqrt{\frac{T_{th}}{T_o}}}{\frac{T_w}{T_o}}\right)^{1/2}$$

$$g_1 = \left(\frac{\sqrt{\frac{A}{A_{th}}} - 1}{\frac{A}{A_{th}}}\right)^{1/2}$$

$$g_2 = \frac{1.73 + 1.11(\gamma - 1)M^2}{M^{1/2}\left(\frac{T}{T_o}\right)^{\frac{3-\gamma}{4(\gamma-1)}}}$$

Equation (B15) must be solved by iteration to account for the change in free-stream conditions in g_2 due to the boundary-layer growth. As a first approximation, equation (B15) may be solved assuming $(A/A_{th})_{eff} = A/A_{th}$. This gives a value of δ^*/r that permits equation (B12) to be solved for $(A/A_{th})_{eff}$, which becomes the basis for the next calculation. If the boundary layer is thin, this process converges rapidly but for thick boundary layers the process is facilitated by using a graphical solution.

REFERENCES

1. Page, R. J.; Buhler, R. D.; Stoner, W. A.; and Masser, P. S.: Arc Plasma Thrustor Studies. Preprint 1508-60, Am. Rocket Soc., Inc., 1960.
2. Greco, Robert V.; and Stoner, Willis A.: Research and Development of a 1-kw Plasmajet Thrustor. AIAA J., vol. 1, no. 2, Feb. 1963, pp. 320-324.
3. King, Charles R.: Compilation of Thermodynamic Properties, Transport Properties, and Theoretical Rocket Performance of Gaseous Hydrogen. NASA TN D-275, 1960.
4. Spisz, Ernie W.: Compilation of Theoretical Rocket Performance for the Chemically Frozen Expansion of Hydrogen. NASA TN D-2080, 1963.
5. Tinling, Bruce E.: Measured Steady-State Performance of Water Vapor Jets for Use in Space Vehicle Attitude Control Systems. NASA TN D-1302, 1962.
6. Bennett, S.; Huss, W.; John, R. R.; and Tuchman, A.: Experimental Propulsion Performance of a Low Power Pulsed Resistojet. Paper No. 65-97, AIAA, 1965.
7. Jack, John R.; Spisz, Ernie W.; and Brinich, Paul F.: Research on Resistance-Heated Hydrogen Thrustors. NASA TN D-2281, 1964.
8. Zucrow, M. J.: Aircraft and Missile Propulsion. Vol. II, John Wiley & Sons, Inc., 1958.
9. Chapman, Dean R.; and Rubesin, Morris W.: Temperature and Velocity Profiles in Compressible Laminar Boundary Layer with Arbitrary Distribution of Surface Temperature. J. Aeron. Sci., vol. 16, no. 9, Sept. 1949, pp. 547-565.
10. Howard, James M.: The Resistojet. ARS J., vol. 32, no. 6, June 1962, pp. 961-962.
11. Bennett, Stewart; Connors, John F.; and Clark, Kenn E.: Development of a 3-Kilowatt Resistojet. Paper No. 64-672, AIAA, 1964.
12. Finke, Robert C.; Holmes, Arthur D.; and Keller, Thomas A.: Space Environment Facility for Electric Propulsion Systems Research. NASA TN D-2774, 1965.
13. Chen, M. M.; Connors, J. F.; John, R. R.; and Megrue, J.: Arc Jet Engine Performance-Experiment and Theory IV. Paper No. 2345-62, ARS, 1962.

"The aeronautical and space activities of the United States shall be conducted so as to contribute . . . to the expansion of human knowledge of phenomena in the atmosphere and space. The Administration shall provide for the widest practicable and appropriate dissemination of information concerning its activities and the results thereof."

—NATIONAL AERONAUTICS AND SPACE ACT OF 1958

NASA SCIENTIFIC AND TECHNICAL PUBLICATIONS

TECHNICAL REPORTS: Scientific and technical information considered important, complete, and a lasting contribution to existing knowledge.

TECHNICAL NOTES: Information less broad in scope but nevertheless of importance as a contribution to existing knowledge.

TECHNICAL MEMORANDUMS: Information receiving limited distribution because of preliminary data, security classification, or other reasons.

CONTRACTOR REPORTS: Technical information generated in connection with a NASA contract or grant and released under NASA auspices.

TECHNICAL TRANSLATIONS: Information published in a foreign language considered to merit NASA distribution in English.

TECHNICAL REPRINTS: Information derived from NASA activities and initially published in the form of journal articles.

SPECIAL PUBLICATIONS: Information derived from or of value to NASA activities but not necessarily reporting the results of individual NASA-programmed scientific efforts. Publications include conference proceedings, monographs, data compilations, handbooks, sourcebooks, and special bibliographies.

Details on the availability of these publications may be obtained from:

SCIENTIFIC AND TECHNICAL INFORMATION DIVISION

NATIONAL AERONAUTICS AND SPACE ADMINISTRATION

Washington, D.C. 20546